

$G\alpha_i$ Controls the Gating of the G Protein-Activated K^+ Channel, GIRK

Sagit Peleg,¹ Dalia Varon,¹ Tatiana Ivanina,¹ Carmen W. Dessauer,² and Nathan Dascal^{1,3}

¹Department of Physiology and Pharmacology
Sackler School of Medicine
Tel Aviv University
Ramat Aviv, 69978
Israel

²Department of Integrative Biology
and Pharmacology
University of Texas
Houston Medical School
Houston, Texas 77030

Summary

GIRK (Kir3) channels are activated by neurotransmitters coupled to G proteins, via a direct binding of $G_{\beta\gamma}$. The role of $G\alpha$ subunits in GIRK gating is elusive. Here we demonstrate that $G\alpha_i$ is not only a donor of $G_{\beta\gamma}$ but also regulates GIRK gating. When overexpressed in *Xenopus* oocytes, GIRK channels show excessive basal activity and poor activation by agonist or $G_{\beta\gamma}$. Coexpression of $G\alpha_{i3}$ or $G\alpha_{i1}$ restores the correct gating parameters. $G\alpha_i$ acts neither as a pure $G_{\beta\gamma}$ scavenger nor as an allosteric cofactor for $G_{\beta\gamma}$. It inhibits only the basal activity without interfering with $G_{\beta\gamma}$ -induced response. Thus, GIRK is regulated, in distinct ways, by both arms of the G protein. $G\alpha_i$ probably acts in its GDP bound form, alone or as a part of $G\alpha\beta\gamma$ heterotrimer.

Introduction

G protein-activated K^+ channels (Kir3, or GIRK) mediate postsynaptic inhibitory effects of various transmitters in atrium and in brain via 7-helix, G protein-coupled receptors (GPCRs). The mediator of neurotransmitter action is $G_{\beta\gamma}$ derived from heterotrimeric G proteins. $G_{\beta\gamma}$ activates GIRK by direct binding (for review, see Yamada et al., 1998). GIRK is also activated by cytosolic Na^+ and membrane phosphatidylinositol 4,5 bisphosphate (PIP_2); the latter is essential for proper GIRK gating by both Na^+ and $G_{\beta\gamma}$ (Logothetis and Zhang, 1999). GIRK family includes five subunits, GIRK1 through GIRK5. Each subunit contains two transmembrane segments, a reentrant P loop, and cytosolic N and C termini. A functional channel is composed of four identical or different subunits. Heterotetrameric GIRK1/GIRK2, GIRK1/GIRK3, and GIRK2/GIRK3 channels are abundant in the brain, and GIRK1/GIRK4 is predominant in the heart (Jelacic et al., 1999; Krapivinsky et al., 1995; Lesage et al., 1995).

All “classical” subtypes of $G\beta$ (1 through 4), tested in combination with several $G\gamma$ subunits, activate GIRK almost equipotently (Lei et al., 2000; Wickman et al., 1994). The $G_{\beta\gamma}$ binding sites are located in the cytosolic

N and C termini of the GIRK subunits (see Huang et al., 1997; Krapivinsky et al., 1998, and references therein). Binding of $G_{\beta\gamma}$ leads to rearrangements in the pore region, altering open channel kinetics and bursting behavior (Sadja et al., 2001; Yi et al., 2001).

$G\alpha$ subunits play an important role in determining the specificity of GPCR-GIRK signaling. In cardiac and neuronal cells, only GPCRs coupled to pertussis toxin (PTX)-sensitive $G\alpha_{i/o}$ proteins activate GIRK (Wickman and Clapham, 1995); the preferred donors of $G_{\beta\gamma}$ are $G\alpha_{i2}$ and $G\alpha_{i3}$ but not $G\alpha_o$ (Kozasa et al., 1996; Sowell et al., 1997). We have previously found that, in excised patches of *Xenopus* oocytes, $G_{\beta\gamma}$ -induced GIRK activation is antagonized by GTP γ S-activated $G\alpha_{i1}$ (but not by $G\alpha_{i2}$ or $G\alpha_{i3}$), and proposed a role for this antagonism in ensuring the specificity of signaling (Schreibmayer et al., 1996). However, later studies showed that, in intact cells, $G_{\beta\gamma}$ released from G_{i1} can activate GIRK (Leaney et al., 2000; Leaney and Tinker, 2000). In all, the role of $G\alpha_i$ in GIRK gating remains uncertain. Also, it is not clear exactly how $G\alpha$ subunits help to determine signaling specificity. Upon overexpression of various components of signaling pathways, such as $G\alpha$ or $G\beta$, GIRK can be activated by $G_{\beta\gamma}$ donated by PTX-insensitive G proteins such as G_s or G_z (Bender et al., 1998; Lim et al., 1995; Sorota et al., 1999; Vorobiov et al., 2000). Thus, factors such as colocalization or scaffolding may be involved in assigning the relevant $G\alpha$ to GIRK. It has been proposed that preformed complexes of GIRK with certain $G\alpha\beta\gamma$ heterotrimers may exist in native cells, assuring fast activation of GIRK by $G_{\beta\gamma}$ derived from these heterotrimers (Hille, 1994; Huang et al., 1995).

In the native tissues, the basal GIRK activity in the absence of activating neurotransmitters is low, and this is believed to be an intrinsic property of the channel (reviewed in Dascal, 1997). However, in *Xenopus* oocytes, the whole-cell basal activity often reaches levels comparable to the agonist-evoked one. Here we demonstrate that, at high levels of channel expression, the basal activity increases at the expense of agonist- or $G_{\beta\gamma}$ -evoked one. We hypothesized that this excessively high basal activity occurred because of a shortage in an endogenous protein needed to keep the basal activity low. Coexpression of $G\alpha_{i3}$ or $G\alpha_{i1}$ restored the normal gating by lowering the basal activity and increasing the level of activation by $G_{\beta\gamma}$, both in intact oocytes and in excised patches, without reducing the total GIRK current or the amount of GIRK protein in the plasma membrane. Our data strongly suggest that $G\alpha_i$ regulates GIRK gating. We propose that $G\alpha_{i-GDP}$, alone or as a part of the $G\alpha\beta\gamma$ heterotrimer, is crucial to keep the channel shut in the absence of an activated GPCR.

Results

Inverse Correlation between Levels of GIRK Expression and the Extent of Activation by Agonist and $G_{\beta\gamma}$

GIRK1/GIRK2 channels were expressed with the muscarinic m2 receptors (m2R) in *Xenopus* oocytes. Whole-

³Correspondence: dascaln@post.tau.ac.il

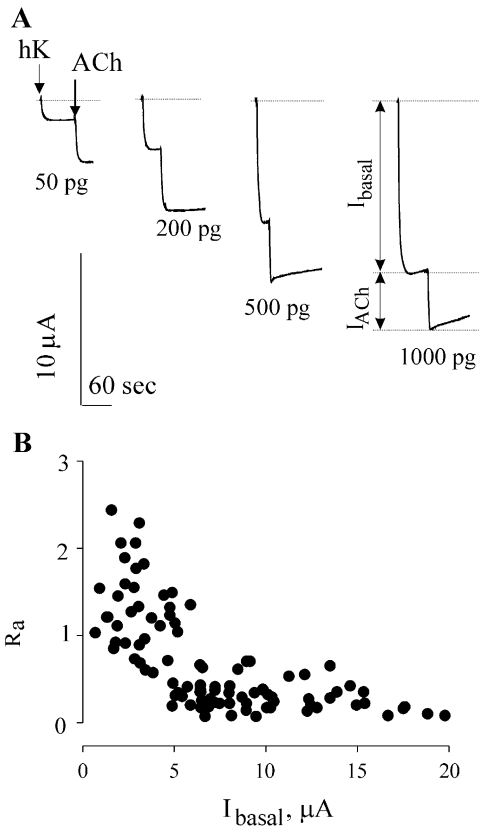


Figure 1. Level of GIRK1/GIRK2 Expression Is Inversely Correlated with the Extent of Activation by Agonist in Intact Oocytes

(A) The dependence of I_{basal} and I_{ACh} on the amount of injected GIRK1 and GIRK2 RNAs (shown below the traces, in pg/oocyte). Solution was switched from ND96 to high K^+ (small arrow), and then to high- K^+ containing $10 \mu\text{M}$ ACh (large arrow). GIRK currents in representative oocytes from one batch are shown.

(B) Summary of experiments in 3 oocyte batches: negative correlation between R_a and I_{basal} measured in the same cell ($p < 0.001$ by Pearce and Spearman tests that assume a linear correlation).

cell currents in intact oocytes were measured using two-electrode voltage clamp. GIRK is an inwardly rectifying channel and conducts little outward K^+ current in a normal physiological (high- Na , low- K) ND96 solution at -80 mV. Upon switching from ND96 to a high- K^+ solution (24 mM K^+), basal inward K^+ current via GIRK channels (I_{basal}) is revealed (Figure 1A). The agonist acetylcholine (ACh) evokes an additional current (I_{ACh}).

When the level (density) of GIRK1/GIRK2 was increased by injecting more RNA of each subunit, I_{basal} became larger, as expected (Figure 1A). In contrast, I_{ACh} did not increase proportionally, and sometimes even decreased at high channel densities. The relative activation by the agonist, R_a , calculated as the ratio ($I_{\text{ACh}}/I_{\text{basal}}$), was strongly reduced as the density of expressed channels increased, and a strong negative correlation between R_a and I_{basal} was revealed (Figure 1B). This phenomenon did not depend on the level of expressed m2R: it was observed either when the amount of the injected m2R RNA was increased proportionally with GIRK, or when m2R RNA was kept constant (500 pg/oocyte).

The inverse relationship between basal activity and R_a was also observed in excised patches when the channel

opening was induced by the addition of purified $\text{G}\beta_1\gamma_2$ protein. In most experiments, GIRK1/GIRK2 was expressed without m2R; the patch pipette contained no agonist. Basal activity was measured as the total open probability of all channels in the patch (NP_o), and corrected for the slight differences in the sizes of the electrodes (Yakubovich et al., 2000) by multiplying by electrode resistance, R_{el} , which is roughly inversely proportional to the patch area. Basal activity was first recorded in the cell-attached (c.a.) configuration. Then the patch was excised into the bath solution, which was devoid of GTP and Na^+ but contained ATP to preserve membrane PIP_2 (Sui et al., 1998). After excision, basal activity decayed by $89.1\% \pm 1.6\%$ ($n = 46$), probably because of lack of Na^+ and GTP in the bathing solution, to a new steady state level within 0.5–2 min (Figure 2A).

Three minutes after the excision, a near-saturating concentration (30–40 nM) of $\text{G}\beta_\gamma$ was added. $\text{G}\beta_\gamma$ caused a strong, several hundred-fold activation at low expression levels (Figure 2A), but much less at high channel densities (Figure 2B). The activation by $\text{G}\beta_\gamma$ (relative to the basal activity recorded in the same excised patch), R_a , showed a strong negative correlation with basal activity (Figure 2C; $n = 47$). For illustration, patches were arbitrarily divided into three groups with low, medium, and high basal NP_o (bar chart in Figure 2C). $\text{G}\beta_\gamma$ -induced activation was about 700-fold in patches with low channel density, but only ~ 22 -fold at high channel density (see also Table 1). The same relationship was observed when the basal activity measured *before* the excision, in the cell-attached configuration, was used for reference: 80-fold activation at low channel density, but only 2.1-fold at high density (Figure 2D). Thus, the factor underlying the inverse correlation between channel density and R_a is retained after patch excision.

The increase in the amount of synthesized channels upon increasing the RNA dose was confirmed by immunocytochemistry (Figure 3A). The total amount of GIRK in whole oocytes, precipitated by a GIRK1 antibody, correlated well with the total GIRK current ($I_{\text{total}} = I_{\text{basal}} + I_{\text{ACh}}$) measured in the same oocyte batch, in a wide range of RNA concentrations (Figure 3B). Both I_{total} and the amount of GIRK protein usually saturated at 1 ng RNA/oocyte. The relationship between the dose of RNA and channel density in the plasma membrane was examined by confocal imaging of the expressed proteins in large flat patches of membrane, attached to cover slips, stained with antibodies at their cytoplasmic surfaces (Singer-Lahat et al., 2000; see also Figure 5). The amount of GIRK1/GIRK2 in the plasma membranes of oocytes injected with 50 or 1000 pg RNA/oocyte, estimated by this method, increased almost exactly as I_{total} in the same two oocyte batches (Figure 3C).

We also verified, using Western blot method, that the amount of $\text{G}\beta_\gamma$ in the total cellular membrane fraction was identical at low and high levels of GIRK; it could be increased only by injecting RNAs encoding $\text{G}\beta$ and $\text{G}\gamma$ (Figure 3D). Furthermore, coexpression of m2R or $\text{G}\alpha_{13}$ also did not substantially alter the level of endogenous $\text{G}\beta_\gamma$ (two experiments; Figure 3E).

Coexpression of $\text{G}\alpha_{13}$ Restores Low I_{basal} and High R_a in Intact Oocytes

A possible interpretation of the above results is that the oocytes contain a limited amount of an endogenous

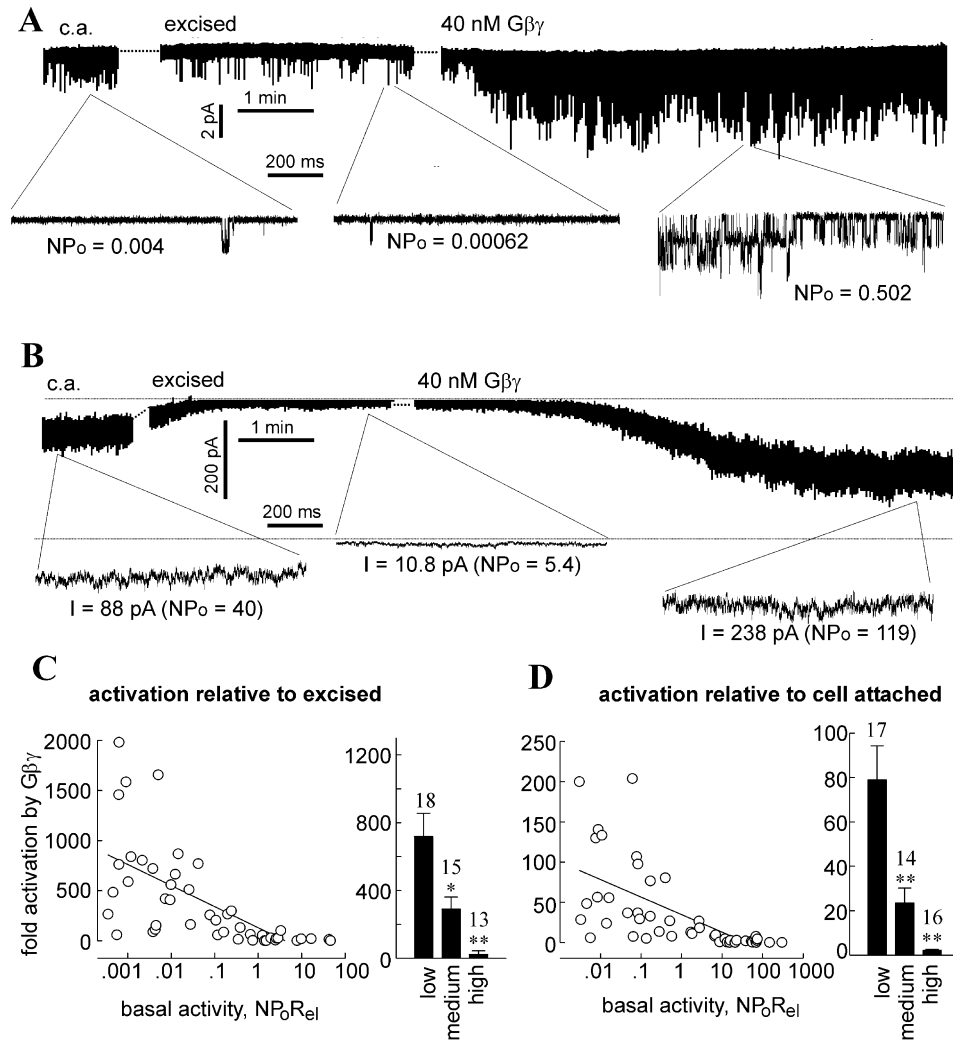


Figure 2. Negative Correlation between the Level of GIRK1/GIRK2 Expression and the Extent of Activation by G $\beta\gamma$ in Excised Patches
(A and B) Typical records in patches from two oocytes from the same donor, injected with 10 (A) or 1000 (B) pg of GIRK1 and GIRK2 RNAs. Upper traces show the time course of the whole experiment (the record during excision and solution mixing was blanked and is shown by dotted lines), lower traces zoom on shorter stretches of record. The horizontal dotted lines show zero current level. At low channel densities, the channel activity was estimated as NP $_o$ (total open probability, which equals number of channels in the patch (N) times the open probability of a single channel (P)). NP $_o$ was calculated from 1 min periods of activity. At high channel densities, total macroscopic currents rather than NP $_o$ were calculated from all-points histograms during 30–60 s periods of activity, and then NP $_o$ was calculated by dividing the macroscopic current (in pA) by the single channel amplitudes estimated in the same experiments (2.2 and 2 pA in c.a. and excised configurations, respectively; data not shown).
(C and D) Relationship between R $_a$ and basal activity in excised (C) or cell-attached (c.a.) (D) configurations. The basal activity of the channel in the excised patches was measured during the third minute after excision. The bar charts show the average R $_a$ in patches arbitrarily divided into groups with low, medium, and high basal current. Basal NP $_o$ R $_{el}$ in these groups was <0.01; 0.01–1; >1, respectively, in excised patches; and <0.1; 0.1–10; >10, respectively, in c.a. patches. *, p < 0.05; **, p < 0.01.

factor (a protein?) that stabilizes a closed resting state of GIRK. At high levels of expression, many channels lack this factor and therefore show higher basal activity and less relative activation by ACh and G $\beta\gamma$. The “lacking” inhibitory molecule may be simply a G α_{13} that sequesters free G $\beta\gamma$ at rest, and serves as G $\beta\gamma$ donor following transmitter-initiated GDP/GTP exchange.

In agreement with this hypothesis, coexpression of G α_{13} reduced I $_{basal}$ and increased I $_{ACh}$ and R $_a$ in intact oocytes (Figure 4A). Interestingly, the more channels were expressed, the more G α_{13} had to be coexpressed in order to reduce I $_{basal}$ and to restore R $_a$, despite the constant level of endogenous G $\beta\gamma$. It looked as if G α_{13}

titrates the channel rather than G $\beta\gamma$. Figure 4B summarizes experiments in which the channel (expressed at either 50 or 1000 pg RNA/oocyte) was titrated by G α_{13} . At 50 pg GIRK RNA, coinjection of 50 pg of G α_{13} RNA did not have any effect, whereas a 10-fold excess of G α_{13} RNA (0.5 ng) reduced I $_{basal}$ by ~60% and increased R $_a$ ~5-fold. In contrast, at high GIRK levels (1000 pg RNA), the same concentration of G α_{13} (0.5 ng RNA) did not significantly affect I $_{basal}$, and R $_a$ was only slightly increased. I $_{ACh}$ increased, but because it was small compared to I $_{basal}$, I $_{total}$ remained practically unchanged. At this high channel density, 5 ng of G α_{13} RNA was needed to reduce I $_{basal}$ and to restore high R $_a$. Note that when

Table 1. The Effect of Purified $G_{\alpha_{11-GTP-\gamma S}}$ on the Activation of GIRK1/GIRK2 Channels, by 30–40 nM $G\beta\gamma$ in Excised Patches

NP_oR_{rel}	R_a without $G_{\alpha_{11-GTP-\gamma S}}$	R_a with 100 pM $G_{\alpha_{11-GTP-\gamma S}}$
<0.01	718 ± 138 (n = 18)	58 ± 55 (n = 6)**
0.01–1	289 ± 73 (n = 15)	220 ± 61 (n = 11)
>1	22.4 ± 7.8 (n = 13)	78 ± 77 (n = 3)

R_a was calculated relative to basal activity in excised patches. **, $p < 0.01$.

the excess of $G_{\alpha_{13}}$ RNA was overwhelming (5 ng $G_{\alpha_{13}}$ versus 50 pg GIRK), both I_{basal} , I_{ACh} and I_{total} were reduced, as expected for a general $G\beta\gamma$ scavenger effect; however, we have also detected a decrease in GIRK protein levels (see Figure 5G).

The effect of $G_{\alpha_{13}}$ at different channel densities was then examined in more detail (Figure 4C). Increasing amounts of channel RNA were injected with matched doses of m2R RNA, with or without a 10-fold excess of RNA of $G_{\alpha_{13}}$. Without $G_{\alpha_{13}}$, increasing the dose of GIRK RNA caused the usual effects: a rise in I_{basal} but less or no increase in I_{ACh} , and a progressive reduction in R_a . Coexpression of $G_{\alpha_{13}}$ reduced I_{basal} at all concentrations. Strikingly, now both I_{basal} and I_{ACh} grew as the channel expression increased, while I_{total} was not changed by coexpression of $G_{\alpha_{13}}$. The negative correlation between channel expression and R_a disappeared; the extent of activation became independent of channel density (Figure 4C). At all doses of GIRK except 50 pg, I_{ACh} was larger in the presence of $G_{\alpha_{13}}$ than in its absence, and the difference progressively increased with RNA dose. This suggests that the small amplitude of I_{ACh} before coexpression of $G_{\alpha_{13}}$ did not reflect a limited amount of

either m2R or endogenous $G\beta\gamma$. I_{total} was also not limited by the availability of endogenous $G\beta\gamma$, as shown by separate experiments, in which coexpression of a large excess of $G\beta\gamma$ (5 or 10 ng $G\beta$ RNA) increased I_{basal} and reduced I_{ACh} but did not change I_{total} either at low (50 pg GIRK RNA) or high (1000 pg RNA) channel densities ($p > 0.2$; data not shown).

Notably, R_a reached 5–15 in the presence of coexpressed $G_{\alpha_{13}}$, well above the values seen at 50 pg GIRK RNA/oocyte (Figures 4B and 4C). High R_a was often observed at lower levels of expression of GIRK (5–25 pg RNA/oocyte; data not shown). We therefore suspect that already at 50 pg GIRK's RNA, endogenous G_{α_i} was not available for all channels.

Our hypothesis predicts that downregulation of endogenous $G_{\alpha_{i/o}}$ should increase I_{basal} and decrease R_a at low channel densities. Indeed, injection of a common $G_{\alpha_{i/o}}$ antisense oligonucleotide increased I_{basal} by 70.7% ± 20.4% and reduced R_a by 57% ± 5.5% when the amount of GIRK RNA was 10–25 pg in two out of three oocyte batches (Figure 4D). Notably, at high channel densities, this effect was absent. In one batch, the oligonucleotide had no effect on I_{basal} or I_{ACh} , possibly because it failed to reduce protein levels of G_{α} . In earlier experiments with GIRK1/GIRK5 channels, antisense oligonucleotides against individual *Xenopus* G_{α} subunits did not affect I_{basal} (Schreibmayer et al., 1996). However, none of them reduced I_{ACh} either (as is expected if a major donor of $G\beta\gamma$ needed for agonist-induced activation is missing). It is possible that, in these experiments, other members of the $G_{\alpha_{i/o}}$ family replaced the subunits knocked down by the antisense treatment.

Control experiments examined the effects of a membrane-attached $G\beta\gamma$ scavenger, c β ARK (myristoylated C

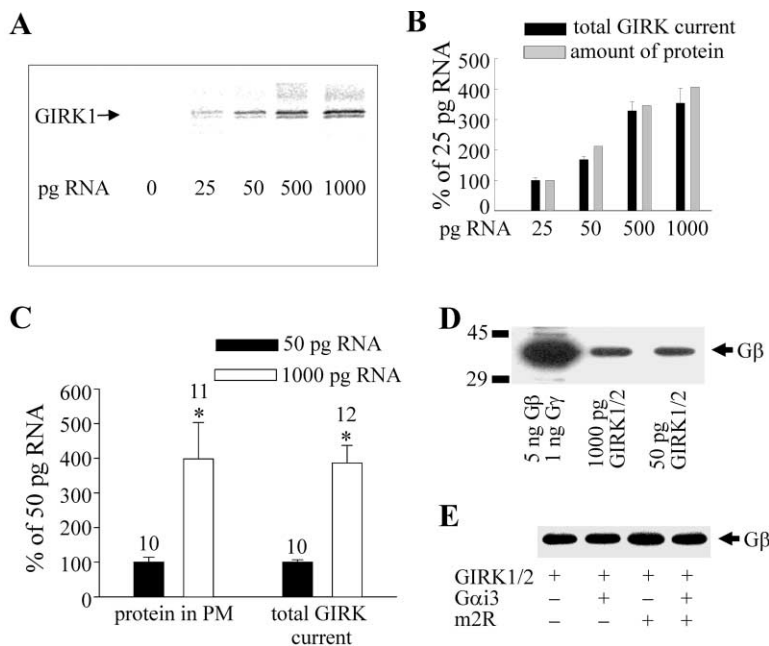


Figure 3. Level of Expression of GIRK1/2 and $G\beta\gamma$, as a Function of RNA Dose

(A) shows immunoprecipitation of [35 S]-labeled GIRK1 from whole oocytes of one donor expressing GIRK1/GIRK2. (B) shows comparison of the amount of GIRK1 protein shown in (A), with I_{total} measured in the same oocyte batch ($n = 5$ oocytes in each group). All parameters were normalized to the reference (25 pg RNA) group. (C) shows comparison of the amount of GIRK1/GIRK2 protein in the plasma membrane measured from the confocal images of GIRK1/GIRK2 in the plasma membrane (exemplified in Figure 5D), and I_{total} in the same batches (summary of two oocyte batches). Numbers of cells tested are shown above the bars. The 50 pg RNA group was taken as reference. *, $p < 0.05$. (D) is a Western blot of $G\beta$ in total cellular membrane fraction of oocytes expressing either GIRK1/GIRK2 (50 or 1000 pg RNA/oocyte) or $G\beta_1\gamma_2$ (5 ng $G\beta_1$ and 1 ng $G\gamma_2$ RNA/oocyte). $G\beta$ was stained with a common $G\beta$ antibody which recognizes $G\beta_1$ through $G\beta_4$. The amount of the endogenous $G\beta$ at 1000 pg GIRK RNA, measured in two such experiments, was 91% and 128% of that measured at 50 pg GIRK. (E) is a Western blot of $G\beta$ in total cellular membrane fraction of oocytes expressing GIRK1/GIRK2 (1000 pg RNA/oocyte) with m2R and/or $G_{\alpha_{13}}$ (0.5 ng and 5 ng RNA/oocyte, respectively).

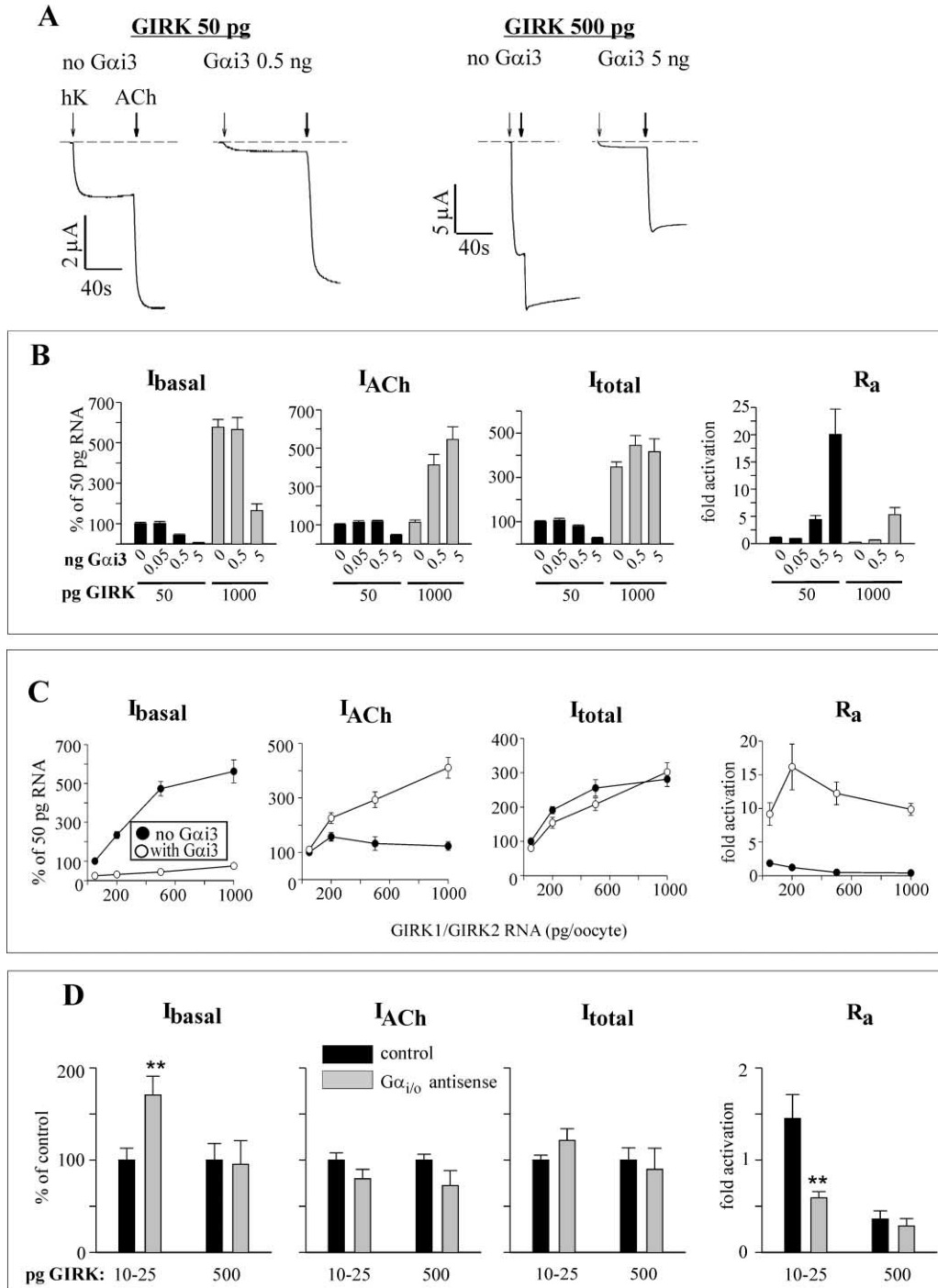


Figure 4. Coexpression of G α_{i3} Restores Low I_{basal} and High I_{ACh}

(A) shows examples of whole-cell GIRK1/2 currents at low (left panel) or high (right panel) channel expression levels, with or without G α_{i3} , recorded in different oocytes of the same batch. Thin arrows denote switch to high-K⁺ solution, thick arrows—addition of ACh. (B) Titration of GIRK by increasing the level of expression of G α_{i3} is shown. Summary from five oocyte batches, 9–28 oocytes in each treatment. The amounts of the RNAs of GIRK and G α_{i3} injected per oocyte are shown at the bottom of the charts. All parameters, except R_a, are shown normalized to the reference group (50 pg GIRK RNA, no G α_{i3}). m2R RNA was injected at 50 pg/oocyte at low GIRK density, and at 500 pg/oocyte at high GIRK density. (C) shows changes in the parameters of GIRK currents in a representative oocyte batch (same as in [A]), as a function of level of GIRK expression, and the effect of G α_{i3} . N = 5 oocytes in each group. All parameters are normalized to the reference group (50 pg GIRK RNA, no G α_{i3}). The amount of m2R RNA was always equal to that of GIRK1, except 1000 pg GIRK RNA when 500 pg of m2R RNA was injected. (D) shows the effect of the antisense G $\alpha_{i/o}$ oligonucleotide on GIRK currents. Fifty nanograms of the oligonucleotide was injected together with the RNAs of m2R (500 pg) and GIRK 3 days before current measurement. In control groups (no oligonucleotide), I_{total} was $1.7 \pm 0.29 \mu\text{A}$ at low channel density (10 or 25 pg GIRK RNA/oocyte, two oocyte batches, n = 10) and $16.6 \pm 2.2 \mu\text{A}$ at high channel density (500 pg GIRK RNA /oocyte, one batch, n = 4). **, p < 0.01.

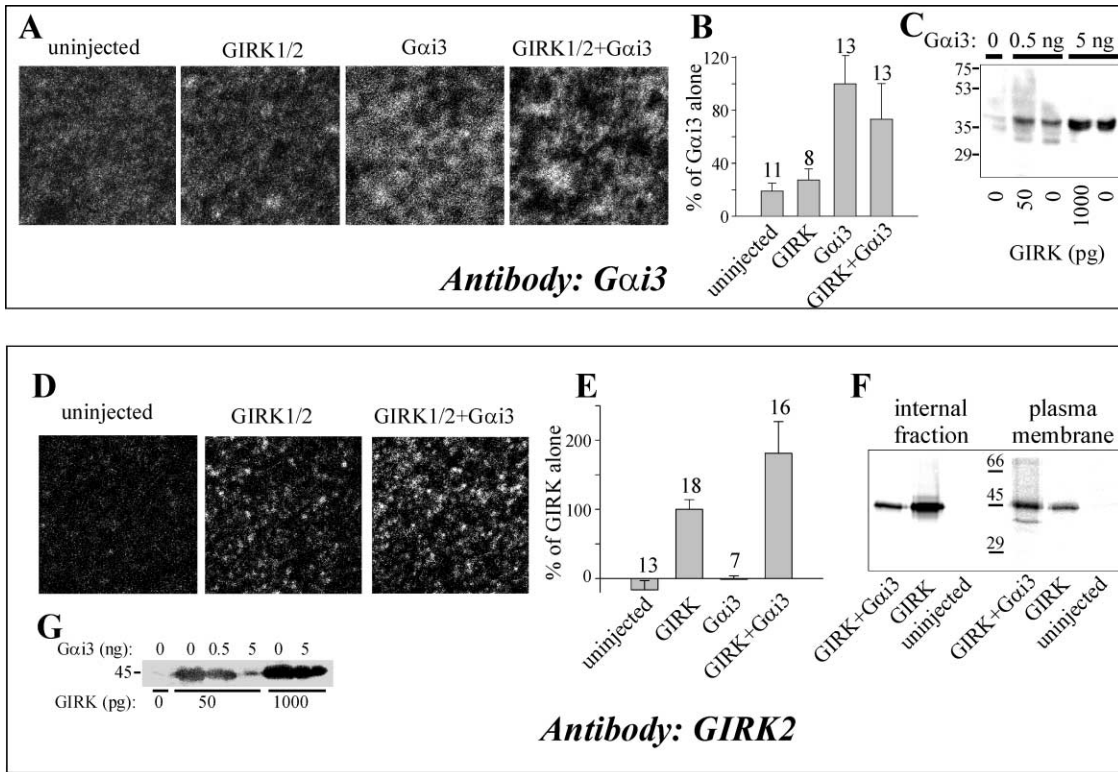


Figure 5. Mutual Effects of GIRK1/2 and $G\alpha_{i3}$ on Each Other's Protein Levels

(A) shows confocal images of $G\alpha_{i3}$ protein in large membrane patches (field: $18 \times 18 \mu\text{m}$). Representative oocytes of one batch. GIRK1/GIRK2 RNA was 1000 pg/oocyte, $G\alpha_{i3}$ 5 ng/oocyte. Endogenous $G\alpha_{i3}$ was also detected by the $G\alpha_{i3}$ antibody in uninjected native oocytes. (B) The amount of $G\alpha_{i3}$ in the plasma membrane is not changed by coexpression of GIRK1/ GIRK 2. Summary of experiments shown in (A) (three batches of oocytes). (C) The total amount of $G\alpha_{i3}$ in the oocytes is not changed by coexpression of GIRK1/GIRK2. Western blot with $G\alpha_{i3}$ antibody (representative of two experiments). Molecular weight markers (in kD) are shown on the left. (D) shows confocal image of GIRK2 in large membrane patches (field: $22 \times 22 \mu\text{m}$). Coexpression of $G\alpha_{i3}$ (5 ng RNA/oocyte) increases the level of GIRK1/2 (1000 pg RNA/oocyte). (E) Summary of the experiments shown in (D), from four oocyte batches, is shown. The increase in GIRK protein by $G\alpha_{i3}$ was statistically significant ($p < 0.05$). (F) shows immunoprecipitation of metabolically [^{35}S]-labeled GIRK channel from oocytes incubated in the presence of [^{35}S]Met/Cys. Plasma membranes from five oocytes were manually separated from the rest of the cell ("internal fraction"), and immunoprecipitated with the GIRK2 antibody. Representative of two experiments. Each sample was done in duplicate (not shown). The plasma membrane contained only about 15% of total GIRK, the rest was in the internal fraction. Therefore, the contrast in the plasma membrane autoradiogram image was increased to enhance the bands. (G) shows a Western blot of $G\alpha_{i3}$ in whole oocytes injected with either 50 or 1000 pg GIRK1/ GIRK2 RNA (as indicated below the image), with or without $G\alpha_{i3}$. The amounts of injected $G\alpha_{i3}$ RNA, in ng/oocyte, are shown above the lanes.

terminus of the β -adrenergic receptor kinase; see Petit-Jacques et al., 1999). In contrast to $G\alpha_{i3}$, coexpressed $c\beta\text{ARK}$ strongly reduced I_{basal} , I_{ACh} , I_{total} , and R_a , at both low and high channel densities (two experiments; data not shown).

We also examined whether $G\alpha_{i3}$ alters GIRK expression, or vice versa. The level of $G\alpha_{i3}$ in the plasma membrane (Figures 5A and 5B) or in whole oocytes (Figure 5C) was not changed by coexpression of GIRK, as estimated by imaging in membrane patches and by Western blotting, respectively. On the other hand, the amount of GIRK in the plasma membrane was mildly increased by coexpression of $G\alpha_{i3}$, as shown by confocal imaging (Figures 5D and 5E) and immunoprecipitation of [^{35}S]-labeled GIRK protein from plasma membranes. Immunoprecipitation showed an 11% and 56% increase in GIRK protein in the presence of $G\alpha_{i3}$ (two experiments; Figure 5F). Interestingly, the total amount of GIRK in the internal fraction was reduced 2- to 4-fold (Figure 5F). This was confirmed by Western blots of whole oocytes

(Figure 5G). The opposite changes in cytosolic and plasma membrane contents of GIRK caused by coexpression of $G\alpha_{i3}$ suggest that $G\alpha_{i3}$ may play a role in the control of GIRK biosynthesis, processing, or transport to membrane.

Coexpression of $G\alpha_{i3}$ Restores Low Basal Activity and High Activation by $G\beta\gamma$ Also in Excised Patches

We next studied the effect of coexpressed $G\alpha_{i3}$ on activation of GIRK by purified $G\beta\gamma$ in excised patches. This protocol bypasses the GPCR and does not rely on $G\beta\gamma$ released from $G\alpha\beta\gamma$ heterotrimers. GIRK was expressed in the absence of m2R, with or without $G\alpha_{i3}$.

Figure 6A shows records from two representative patches from oocytes of the same donor. When the channel was expressed alone at high density (1000 pg RNA), the basal activity in cell-attached configuration and after the excision was high, and relative activation by $G\beta\gamma$ was rather poor (Figure 6A, upper trace; see

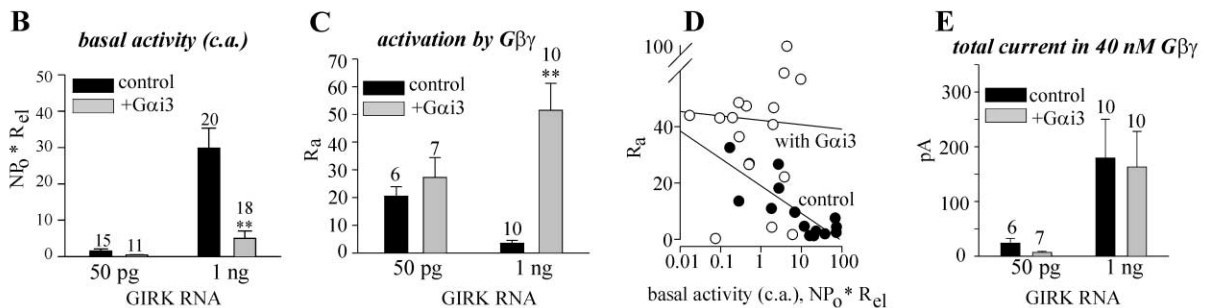
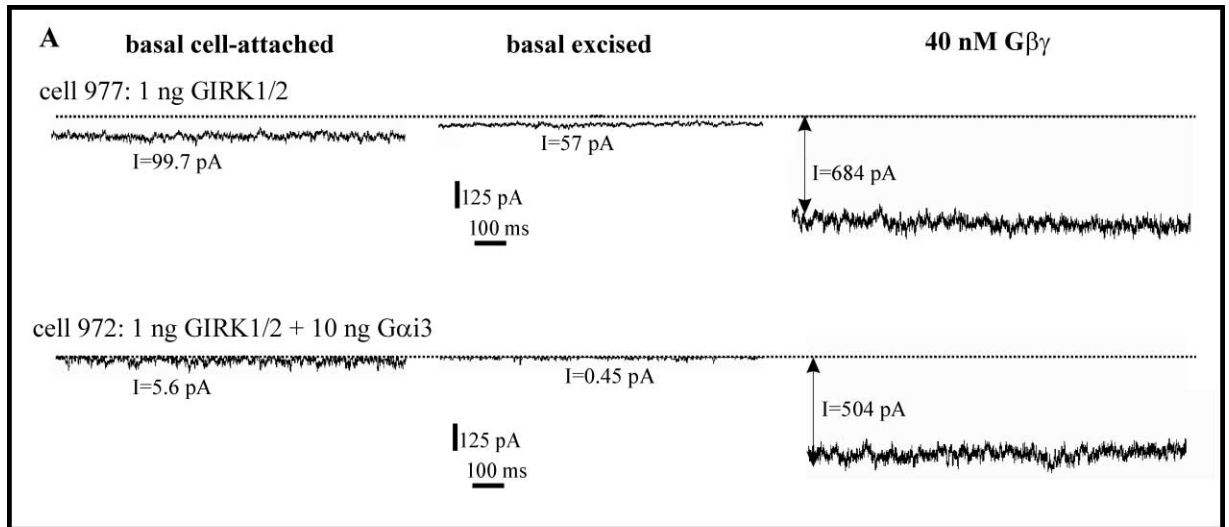


Figure 6. G α_{i3} Normalizes the Gating of GIRK1/GIRK2 in Excised Patches

GIRK was expressed at 50 or 1000 pg/oocyte. G α_{i3} RNA was injected in 5- or 10-fold excess over GIRK1/GIRK2. The protocol and solutions were as in Figure 2. (A) shows representative records from patches in two oocytes of the same batch. (B–E) summary of a series of experiments in four oocyte batches is shown. Comparison of the parameters of GIRK gating with or without G α_{i3} : basal c.a. activity (B); extent of activation by G $\beta\gamma$ (R_a) (C); the correlation between R_a and basal activity (D); and the total current in 40 nM G $\beta\gamma$ (E). ** indicates $p < 0.01$. Linear regression lines in (D) are shown for illustration only.

Figure 6C for a summary). Coexpression of a 5- or 10-fold excess of G α_{i3} RNA did not change single-channel conductance (data not shown) or the extent of decay of basal activity after patch excision. With and without G α_{i3} , the decay was $89.7\% \pm 3.9\%$ ($n = 6$) and $80\% \pm 4.5\%$ ($n = 7$) at 50 pg, and $77.6\% \pm 5.3\%$ ($n = 10$) and $81\% \pm 2.6\%$ ($n = 10$) at 1000 pg GIRK RNA. However, coexpression of G α_{i3} strikingly reduced basal activity and improved the relative activation by 40 nM G $\beta\gamma$ (Figure 6A, compare upper and lower traces).

A summary of this series of experiments is shown in Figures 6B–6E (cell-attached basal currents were used for reference). The effects of G α_{i3} were strikingly similar to those observed in whole cells (where channel was activated via m2R): G α_{i3} strongly reduced the basal activity (Figure 6B) and greatly increased R_a (Figure 6C) at high channel density, with much milder effects at low channel density. The negative correlation between basal activity and R_a in the absence of G α_{i3} ($p = 0.029$ by Pearson correlation analysis) disappeared after coexpression of G α_{i3} ($p = 0.875$; Figure 6C). The total GIRK current in the presence of G $\beta\gamma$ was not reduced by coexpression of G α_{i3} ; thus, coexpressed G α_{i3} did not impair activation by G $\beta\gamma$ (Figure 6D). These results support the

role for G α_{i3} as the factor needed for a proper, low basal activity and a strong activation by G $\beta\gamma$.

To examine in detail whether G α_{i3} acts as a scavenger or an allosteric regulator of G $\beta\gamma$, we have recorded a full dose-response relation for G $\beta\gamma$ activation (Figure 7A). GIRK was expressed alone (1000 pg RNA) or with G α_{i3} (5 ng RNA), or with c β ARK (5 ng RNA). R_a was calculated relative to basal activity in excised patches, to facilitate comparison with earlier works. The half-maximal activation of the channel expressed alone occurred at about 10 nM G $\beta\gamma$, similarly to GIRK1/GIRK4 channels (Wickman et al., 1994). G α_{i3} did not substantially change the apparent affinity of G $\beta\gamma$, but greatly increased the maximal level of activation. The absence of a rightward shift of the dose-response curve by coexpressed G α_{i3} supports the notion that G α_{i3} did not substantially sequester the added G $\beta\gamma$ under the conditions used. In contrast, c β ARK strongly reduced activation at all G $\beta\gamma$ concentrations; some activation was apparent at 80 nM, suggesting that the dose-response curve was shifted to the right, as expected for a G $\beta\gamma$ scavenger.

To inquire what happens when the supply of endogenous G α_i is presumably sufficient, we expressed GIRK at low levels (5–10 pg RNA/oocyte). Many patches con-

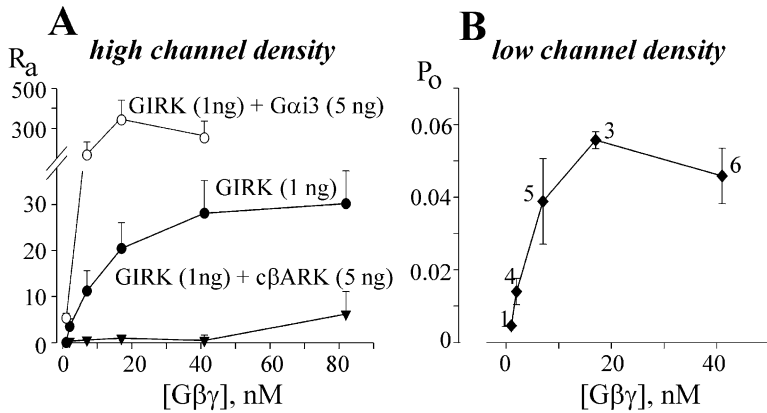


Figure 7. Dose-Response Relationships for Gβγ Activation of GIRK1/GIRK2 at High and Low Expression Levels, and the Effect of Coexpression of Gαi3 and cβARK

In most patches, only one or two concentrations of Gβγ have been tested. (A) shows Gβγ dose-response at high channel densities (1000 pg RNA/oocyte), and the effect of coexpression of cβARK or Gαi3. Summary of a separate series of experiments in four oocyte batches. Each point on each curve is mean ± SEM from 4–8 patches. (B) shows Gβγ dose-response at low channel densities (5 or 10 pg GIRK RNA/oocyte). Summary from three oocyte batches is shown. Po was calculated per single channel, by dividing NPo by number of channels (N) estimated from the maximum

number of overlaps. Only patches with ≤4 channels were used, to avoid mistakes in estimating channel number (Yakubovich et al., 2000). Number of patches tested at each concentration is indicated near each point.

tained only one channel, and the basal activity was too low to be reliably estimated; thus, single-channel Po was calculated instead of Ra. The half-maximal activation dose of Gβγ was similar to that at high channel densities (Figure 7B). In five patches in which the basal activity after excision could be reliably measured, maximal Ra was 301 ± 141, similar to the level of activation obtained with high channel densities in the presence of Gαi3 (compare with Figure 7A).

Purified Gαi1-GDP Inhibits the Basal Activity of GIRK Expressed at High Densities

Coexpressed Gαi3 probably acted in excised patches in its GDP bound form because we used GTP-free bath solution (see Discussion). To confirm the ability of Gαi-GDP to reduce Ibasal of overexpressed GIRK, we used purified Gαi1-GDP. First, we verified that, in whole oocytes, coexpressed Gαi1 acted like Gαi3 (Figure 8A; compare with Figure 4B); it strongly reduced Ibasal and increased IACH

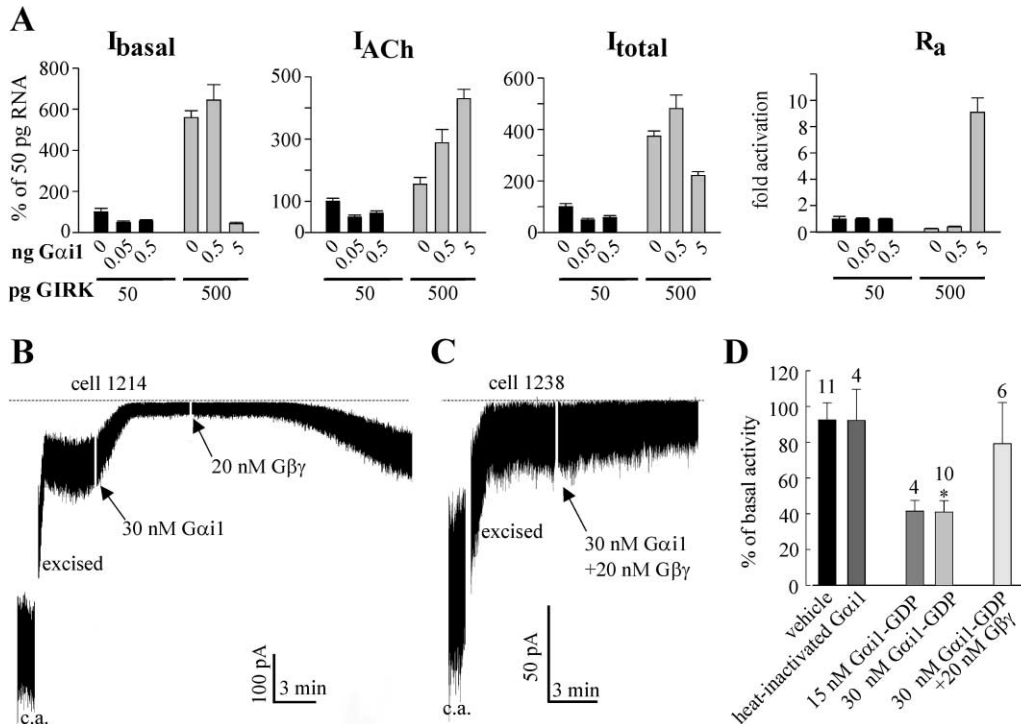


Figure 8. Purified Gαi1 Inhibits Basal Activity of GIRK

(A) Coexpression of Gαi1 reduces whole-cell Ibasal and increases Ra, similarly to Gαi3 (same protocol as in Figure 4B, except that the amount of injected m2R RNA was 500 pg/oocyte in all groups). One oocyte batch; n = 5 in all groups. (B and C) show effects of purified Gαi1-GDP and Gβγ in representative excised patches. Dotted lines show zero current level. Gαi1-GDP was applied before Gβγ (B) or after pre-mixing with Gβγ (C). (D) shows summary of experiments in (B) and (C). The basal NPo was calculated for a 1 min period between 2nd and 3rd min after patch excision. The effect of Gαi1-GDP or the Gαi1-GDP-Gβγ mixture was measured between 2nd and 3rd min after the addition. Vehicle: 1 μl of the Gα storage buffer, added in the same way as the purified proteins (see Experimental Procedures). *, p < 0.01.

and R_a at high channel densities. Then the effect of purified myristoylated recombinant G α_{i1-GDP} was examined in excised patches, with GIRK1/GIRK2 expressed at 500–1000 pg RNA/oocyte. Channel activity was first measured in c.a. configuration. Excision into the Na⁺- and GTP-free medium caused the usual decay of NP_o followed by stabilization (Figure 8B). Three to four minutes after excision, 30 nM G α_{i1-GDP} was added; this caused a 59.1% \pm 6.4% decrease in I_{basal} within 3 min (n = 10, p = 0.006; Figures 8B and 8D). Vehicle or heat-inactivated G α_{i1-GDP} were without effect (Figure 8D). Addition of 20 nM G $\beta\gamma$ after 30 nM G α_{i3} increased NP_o 6.7- \pm 2.0-fold over the pre-G $\beta\gamma$ level (n = 9; Figure 8B). In the control group (vehicle), addition of G $\beta\gamma$ appeared to produce a stronger activation, 14.2- \pm 5.8-fold, though the difference was not statistically significant (n = 11; p > 0.2). Given a dissociation constant of the heterotrimeric G $\alpha\beta\gamma$ complex of 2–8 nM (Sarvazyan et al., 1998), a mixture of 30 nM G α_{i1} and 20 nM G $\beta\gamma$ should contain 2.8–6.5 nM free G $\beta\gamma$. Mild activation by this residual free G $\beta\gamma$ is reasonable, and it is indeed expected to be less than with 20 nM G $\beta\gamma$ alone (see G $\beta\gamma$ dose-response in Figure 7). Sixty nanomolar G α_{i1-GDP} practically prevented activation by 20 nM G $\beta\gamma$ (calculated 0.7–3 nM free G $\beta\gamma$; data not shown).

We also examined the effect of addition of G α_{i1-GDP} and G $\beta\gamma$ (30 nM + 20 nM, respectively) pre-mixed at room temperature for 2 min in 50 μ l bath solution. This mixture is expected to contain roughly 15 nM G $\alpha_{i1-GDP}\beta\gamma$ heterotrimer and about 15 nM free G α_{i1-GDP} . In 3 out of 6 patches, this mixture produced initial inhibition within the first 3 min, but, on the average, the basal activity was not significantly affected (Figures 8C and 8D). Mild activation sometimes occurred later; an average level of 2.4 \pm 1.3-fold above basal was eventually reached (n = 6). This is comparable to the maximal channel activity reached in the experiments of Figure 8B after the addition of G $\beta\gamma$, relative to basal activity measured *before* the addition of G α_{i1-GDP} (2.7 \pm 1-fold, n = 9). In comparison, 15 nM G α_{i1-GDP} alone inhibited the basal GIRK current almost as well as 30 nM G α_{i1-GDP} (Figure 8D). These results support the idea that G α_{i1-GDP} alone is able to downregulate the basal GIRK activity and, as yet, do not indicate an outstanding inhibitory effect of the G $\alpha\beta\gamma$ heterotrimer.

The Inhibitory Effect of Purified, GTP γ S-Activated G α_{i1} on GIRK Activation Depends on Channel Density

The above results suggest that the basal activity can be regulated by G α_{i-GDP} ; they are not directly related to the previously reported attenuation of G $\beta\gamma$ -induced activation by low concentrations of purified GTP γ S-activated G α_{i1} , 25–100 pM (Schreibmayer et al., 1996; Yakubovich et al., 2000). These earlier studies utilized low expression levels of GIRK1/GIRK5 and GIRK1/GIRK4 channels. We have found that G $\alpha_{i1-GTP\gamma S}$ inhibited G $\beta\gamma$ -induced activation of GIRK1/GIRK2, too, but only at very low channel densities (Table 1). Therefore, it is possible that the effect of purified G $\alpha_{i1-GTP\gamma S}$ depends on the presence of an endogenous protein which is lacking at high channel expression levels. One possibility is that, in excised patches, the added G $\alpha_{i1-GTP\gamma S}$ somehow interferes with the normal gating effect of an endogenous G α . At

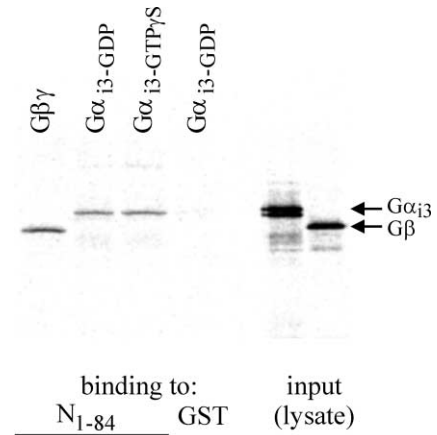


Figure 9. In Vitro Synthesized G α_{i3} Binds to the N Terminus of GIRK1
Five microliters of reticulocyte lysate containing [³⁵S]-labeled G α_{i3} was incubated with N₁₋₈₄ or GST in the presence of 100 μ M GDP or GTP γ S. [³⁵S]-labeled G $\beta\gamma$ was incubated similarly but without the guanine nucleotides. The GST fusion protein (and the proteins bound to it) was pulled down by binding to glutathione Sepharose affinity beads, eluted with 15 mM glutathione, and separated on agarose gel. G α_{i3} and G $\beta\gamma$ were visualized using PhosphorImager. The two right bands show the labeled proteins in the lysate (before the reaction with N₁₋₈₄); 1 μ l of 1:20 diluted lysate was loaded onto each lane.

present, we also cannot discard the possibility that an unknown contaminant in our preparation of G $\alpha_{i1-GTP\gamma S}$ could have caused the inhibitory effect, but it could not be G α_{i1-GDP} since at 100 pM, the latter did not inhibit activation of GIRK by 20–40 nM G $\beta\gamma$ (Schreibmayer et al., 1996, and data not shown).

G α_{i3} Directly Interacts with GIRK1

Huang et al. (1995) observed direct binding of purified G α_{i1} to the N terminus of GIRK1. To examine whether G α_{i3} also interacts with GIRK1, we constructed a GST-fused N-terminal segment, N₁₋₈₄, and measured its binding to in vitro synthesized, [³⁵S]-methionine-labeled G α_{i3} in the presence of either GDP or GTP γ S. Figure 9 demonstrates that both GDP and GTP γ S bound forms of G α_{i3} interact with N₁₋₈₄. The GDP bound G α_{i3} showed slightly less binding compared to G $\alpha_{i3-GTP\gamma S}$ (69% \pm 11%, n = 5). As reported previously (Huang et al., 1995), G $\beta\gamma$ also bound to the same GST fusion protein, showing about 2-fold stronger binding than G α_{i3} (Figure 9).

Discussion

We have demonstrated that G α_i regulates the gating of GIRK. The regulation is membrane delimited, and G α_{i3} directly binds to GIRK1, but it is not clear yet whether this direct interaction mediates the effects of G α_{i3} . The main function of G α_i is to stabilize the low basal activity of the GIRK channel, in effect “priming” it for G $\beta\gamma$ activation.

An Extrinsic Factor Is Required to Maintain the Low Basal Activity of GIRK

Basal GIRK activity is known to depend on free G $\beta\gamma$ present in the cells due to background GDP/GTP ex-

change at G_{α} (reviewed in Dascal, 1997). Low basal GIRK conductance in native tissues is important to ensure robust activation by agonists and high signal-to-noise ratio in GIRK signaling. In the atrium, only rare single GIRK openings are seen at rest. ACh (added to the external side of the membrane) or purified $G_{\beta\gamma}$ (added to the cytosolic side of the membrane in excised patches) cause robust activation characterized by frequent bursts of opening (Ivanova-Nikolova and Breitwieser, 1997; Sakmann et al., 1983). This pattern of opening is preserved in *Xenopus* oocytes expressing relatively low amounts of GIRK1/GIRK4 (Kim et al., 1997; Nemeč et al., 1999; Petit-Jacques et al., 1999; Yakubovich et al., 2000) or GIRK1/GIRK2 (Figure 2). However, the reported values of the extent of activation by 20–40 nM of $G_{\beta\gamma}$ in excised patches vary considerably, from 12-fold (Petit-Jacques et al., 1999; see their Figure 2) to almost 800-fold (Yakubovich et al., 2000). Here we demonstrate that the extent of activation of GIRK (relative to basal activity) by purified $G_{\beta\gamma}$ or ACh, R_a , is dramatically reduced at high channel densities. The negative correlation between R_a and channel density was observed in GIRK1/GIRK2 (this report) and also in the atrial type GIRK1/GIRK4 channels (S.P. and N.D., unpublished observations).

The hypothesis that we have put forward to explain these observations was as follows: the basal activity depends not only on $G_{\beta\gamma}$, but also on the presence of a factor which opposes the activating effect of $G_{\beta\gamma}$ and helps to keep I_{basal} low. This factor is of limited supply in the oocyte. It is preserved in excised patches, therefore it must be anchored to the membrane or to the channel. It lies downstream of the neurotransmitter receptor, because the inverse relationship between channel density and R_a takes place in excised patches, where GIRK is activated by purified $G_{\beta\gamma}$ which bypasses the receptor. At high channel densities, there is a shortage in this factor, and the basal activity rises *at the expense of the evoked one*. This explains the decrease in the extent of activation by ACh or $G_{\beta\gamma}$.

Several alternative explanations of the observed phenomena can be ruled out.

(1) “Insufficient” activation by ACh at high channel densities, contrasting the strong activation at low channel densities, could be due to insufficient amount of expressed m2R or endogenous $G_{\beta\gamma}$. The strongest argument against this possibility is the poor activation of GIRK in excised patches, at high channel densities, by saturating concentrations of *added* $G_{\beta\gamma}$ (which acts directly on the channel, bypassing m2R). Also, large I_{ACh} and high R_a were restored by coexpression of $G_{\alpha_{i3}}$, without changing the amount of the receptor or the level of $G_{\beta\gamma}$. Even at the highest channel densities attained in our experiments, the total GIRK current ($I_{\text{total}} = I_{\text{basal}} + I_{\text{ACh}}$) was not increased by coexpression of $G_{\beta\gamma}$, suggesting that there was enough $G_{\beta\gamma}$ for maximal activity. The only factor that limited I_{total} in our experiments was the amount of expressed channels in the plasma membrane. I_{total} was a reliable indicator of the relative channel density in the plasma membrane (Figure 3).

(2) Overexpression of GIRK could have increased the levels of endogenous $G_{\beta\gamma}$ in the oocyte. This would increase basal GIRK activity at the expense of the agonist-evoked one (Lim et al., 1995; Reuveny et al., 1994).

However, direct measurements of G_{β} protein levels showed that overexpression of GIRK did not alter the amount of $G_{\beta\gamma}$ in the cell (Figure 3). The mass law dictates, then, that there would be *less* $G_{\beta\gamma}$ *per channel* as the number of channels increases, even if overexpressed GIRKs effectively recruit $G_{\beta\gamma}$ to their vicinity. Thus, if anything, a *lower* I_{basal} would be expected if $G_{\beta\gamma}$ were the only factor determining I_{basal} .

(3) Formation of channel oligomers or clusters, upon overexpression of GIRK, could hinder the access of $G_{\beta\gamma}$ to the channels. This is unlikely because $G_{\beta\gamma}$ finds its way to the channels and activates them well after coexpression of $G_{\alpha_{i3}}$, although the latter does not reduce the density of GIRK in the membrane.

G_{α_i} Is a Candidate Factor Regulating the Basal Activity of GIRK

We propose that the hypothetical factor that is lacking at high channel densities is a G_{α} subunit, possibly of the $G_{\alpha_{i/o}}$ class. The main observations that support this hypothesis are (1) Coexpression of $G_{\alpha_{i3}}$ reduces the basal activity and restores the efficient activation by ACh and $G_{\beta\gamma}$. It eliminates the negative correlation between basal activity and R_a ; the factor (or a lack of such) that caused this effect has gone. (2) Our hypothesis predicts that coexpression of G_{α} should improve agonist- or $G_{\beta\gamma}$ -induced activation mainly at high channel densities, when the lack of endogenous G_{α} is more severe; this was indeed observed (Figures 4C, 6C, and 8). (3) The restoration of correct gating by coexpressed $G_{\alpha_{i3}}$ takes place both in intact cells and in excised patches. Thus, $G_{\alpha_{i3}}$ acts by a membrane-delimited mechanism; this is what we also find regarding the hypothetical “lacking” factor. (4) Antisense knockdown of endogenous $G_{\alpha_{i/o}}$ increases I_{basal} and reduces R_a at low channel densities, compatible with an important role of endogenous $G_{\alpha_{i/o}}$ in keeping the basal activity low. (5) Purified $G_{\alpha_{i1-GDP}}$ inhibits the basal activity of the overexpressed GIRK in excised patches. Again, this is a membrane-delimited regulation; although not conclusive, it is in line with an inhibitory role for G_{α_i} .

Coexpressed G_{α_i} Is Not Only a Simple Scavenger of $G_{\beta\gamma}$; It Also Regulates Gating

$G_{\alpha_{iGDP}}$ binds $G_{\beta\gamma}$ with high affinity, and coexpression of $G_{\beta\gamma}$ is often used to “sequester” free $G_{\beta\gamma}$, preventing it from interacting with its effectors. $G_{\alpha\beta\gamma}$ heterotrimers also serve as donors of $G_{\beta\gamma}$ if activated by relevant GPCRs. In the case of GIRK, coexpression of G_{α_i} is expected to sequester free $G_{\beta\gamma}$ and reduce I_{basal} at rest, and to release $G_{\beta\gamma}$ after activation of m2R by ACh, causing a larger I_{ACh} . However, this trivial acceptor/donor scenario fails to account for several key observations (except when G_{α} is expressed in great excess over GIRK, and reduces I_{total}).

The strongest argument against this simple model is the ability of coexpressed $G_{\alpha_{i3}}$ to restore strong activation by *artificially added* $G_{\beta\gamma}$ in excised patches ($G_{\alpha_{i3}}$ “primes” the channel for activation by $G_{\beta\gamma}$). In this paradigm, $G_{\alpha_{i3}}$ is not a donor of $G_{\beta\gamma}$; in the simple model, it is actually expected to sequester the added $G_{\beta\gamma}$, reducing the activation. Furthermore, coexpressed $G_{\alpha_{i3}}$ did not reduce the apparent $G_{\beta\gamma}$ affinity, despite a great

reduction in basal activity; activation by G $\beta\gamma$ was enhanced. These effects are in stark contrast to those of a typical G $\beta\gamma$ scavenger, c β ARK (Figure 7), and incompatible with a simple G $\beta\gamma$ scavenger effect. Rather, G α_i seems to stabilize a closed “basal” conformation of the channel, by acting alone or in concert with G $\beta\gamma$. Whole-cell data support this impression: the correlation between the channel density and the amount of G α_i , that had to be expressed to reduce I_{basal} and increase R_a , was the first hint to suggest that the effect of G α_{i3} may depend on its interaction with the channel.

G $\beta\gamma$ and G $\alpha_{i\text{-GDP}}$ Regulate GIRK in Distinct Ways

The enhancement of G $\beta\gamma$ activation by coexpressed G α_{i3} is only relative to basal activity; the lack of a significant shift in G $\beta\gamma$ dose-response curve by coexpressed G α_{i3} suggests that G α_{i3} does not act as a strong positive allosteric regulator for G $\beta\gamma$. G α_{i3} regulates the basal activity of the channel but does not interfere with the activation caused by G $\beta\gamma$. Thus, GIRK is regulated by both G α and G $\beta\gamma$, like adenylyl cyclases and phospholipases C (Clapham and Neer, 1997; Sunahara et al., 1996). The two arms of the G protein pathway have distinct effects on GIRK gating.

In the resting cells, all three forms of G α coexist: free G α_{GTP} , free G α_{GDP} , and G $\alpha_{\text{GDP}}\beta\gamma$ heterotrimer (Gilman, 1987; Ross, 1995; Sarvazyan et al., 1998). The orthodox view is that only G α_{GTP} is the “active” form of G α that regulates various effectors. However, we have observed that the inhibitory effect of coexpressed G α_{i3} on the basal activity persists for many minutes after patch excision in the absence of GTP in the solution. All GTP bound to free G α_i would be hydrolyzed within this time by the intrinsic GTPase activity of G α (Ross, 1995). Therefore, GIRK appears to be regulated by G α_{GDP} or the G $\alpha_{\text{GDP}}\beta\gamma$ heterotrimer.

It is possible that direct binding of G $\alpha_{i\text{-GDP}}$ (or G $\alpha_{\text{GDP}}\beta\gamma$) to GIRK is sufficient to reduce the basal activity. However, more complex anchor/donor schemes are plausible; in order to be viable, they must incorporate the assumption of a direct G α_i (or G $\alpha\beta\gamma$)-GIRK interaction. For instance, the N terminus of GIRK1 may be part of the channel’s G protein anchoring site (Huang et al., 1995) and also a part of a high-affinity G $\beta\gamma$ binding site that regulates the basal activity and is separate from the low-affinity C-terminal G $\beta\gamma$ binding site which underlies the activation by agonist (He et al., 1999). In this case, binding of G α at this site may provide an anchor for G $\beta\gamma$, to be released when an agonist-activated GPCR arrives. It will prevent G $\beta\gamma$ from activating the channel via this site, reducing the basal activity, but it will not interfere with G $\beta\gamma$ activation via the separate low-affinity G $\beta\gamma$ site. A somewhat different scheme is one in which the affinity of the heterotrimeric G $\alpha\beta\gamma$ toward the channel is higher than that of G $\beta\gamma$ or G α_i alone. At low channel densities, most channels will be associated with G $\alpha\beta\gamma$ and have low basal activity. If the concentration of free G $\beta\gamma$ in oocytes is higher than that of free G α and/or the heterotrimer (see, for instance, Lutz et al., 2000), then at high channel densities, many channels will lack the heterotrimer and have a high basal activity due to the binding of free G $\beta\gamma$. Coexpressed G α , or added purified G α -GDP, will bind G $\beta\gamma$, and the newly formed hetero-

trimer will restore normal gating parameters. Although our present results (Figure 8) do not favor the idea of a crucial role for heterotrimeric G $\alpha\beta\gamma$ as the main negative regulator of basal activity, experiments with purified G protein subunits are complicated by the inevitable presence of a mixture of free G α -GDP, G $\beta\gamma$, and G $\alpha\beta\gamma$ in the bath solution. Thorough titration of these ingredients and comparison of their effects may help to better understand their relative roles in the control of basal activity of GIRK. These and other future studies are hoped to clarify whether the direct binding of G α_i contributes to its effect on gating, and whether its effect takes place within a complex scheme in which G $\beta\gamma$ is also involved.

Experimental Procedures

cDNA Constructs and mRNA

The coding sequences of all cDNAs used in this study were obtained or prepared as described in our previous publications (Sharon et al., 1997; Vorobiov et al., 2000). All cDNAs were inserted into high-expression oocyte vectors containing 5' and 3' untranslated sequences of *Xenopus* β -globin: pGEMHE or its derivative pGEMHJ, or pBS-MXT. mRNAs were synthesized in vitro (see Yakubovich et al., 2000). The antisense G α_{i0} oligonucleotide (G $^{\text{S}}$ G $^{\text{S}}$ T $^{\text{S}}$ CCTTGAAAG TGAAG $^{\text{S}}$ T $^{\text{S}}$ G $^{\text{S}}$, where $^{\text{S}}$ denotes a phosphothiol group), shared the following % homology with cDNA sequences of known *Xenopus* G α proteins: G α_{i1} , 90; G α_{i2} , 90; G α_{i3} , 100; G α_{i0} , 84; G α_{q} , 48; G α_s , 37; G α_{14} , 58.

Oocytes and Electrophysiology

Xenopus laevis frogs were maintained and operated, and the oocytes were prepared and injected with RNA as described (Yakubovich et al., 2000). After RNA injection, oocytes were incubated for 3 to 5 days at 20–22°C in ND96 solution (96 mM NaCl, 2 mM KCl, 1 mM MgCl $_2$, 1 mM CaCl $_2$, 5 mM HEPES, pH 7.5), supplemented with 2.5 mM Na pyruvate and 50 μ g/ml gentamycin.

Data acquisition and analysis were done using the Axotape and the pCLAMP software (Axon Instruments Inc., Foster City, CA). All experiments were done at 20–22°C. Whole-cell GIRK currents were measured using two-electrode voltage clamp (Sharon et al., 1997) at –80 mV in a high-K $^+$ solution containing 24 mM KCl, 72 mM NaCl, 1 mM CaCl $_2$, 1 mM MgCl $_2$, 5 mM Hepes (pH = 7.5).

Patch clamp experiments were done as described (Schreibmayer et al., 1996; Yakubovich et al., 2000). Currents were recorded at –80 mV, filtered at 2 kHz, and sampled at 5 or 10 kHz. Patch pipettes had resistances of 0.8–2.5 M Ω . Pipette solution contained, in mM: 144 KCl, 2 NaCl, 1 MgCl $_2$, 1 CaCl $_2$, 1 GdCl $_3$, 10 Hepes/KOH, pH 7.5. GdCl $_3$ completely inhibited the stretch-activated channels. Bath solution contained, in mM: 130 KCl, 2 MgCl $_2$, 1 EGTA, 2 Mg-ATP, 10 Hepes/KOH, pH 7.5. After seal formation, the patches were excised and exposed to air to prevent the formation of closed membrane vesicles at the tip. See legend to Figure 2 for additional details.

Purified recombinant G $\alpha_{i1\text{-GDP}}$, G $\alpha_{i1\text{-GTP}}\gamma_s$, and G $\beta_1\gamma_2$ were prepared and used as described (Schreibmayer et al., 1996; Yakubovich et al., 2000). Stock solutions of the purified G protein subunits were diluted into 50 μ l of the bath solution, added to the 500 μ l solution in the bath, and stirred. Purified myristoylated G $\alpha_{i1\text{-GTP}}\gamma_s$ was stored in aliquots at 2.5–20 μ M and used within 2–3 months after activation with GTP γ S; loss of activity (assayed by inhibition of G $\beta\gamma$ -induced activation of GIRK1/GIRK5 or GIRK1/GIRK2 expressed at a low density) was observed upon longer storage at –80°C. After thawing at 30°C, an aliquot was kept on ice, diluted into bath solution, and used within no more than 5 min. Purified myristoylated G $\alpha_{i1\text{-GDP}}$ (20–30 μ M) was stored similarly but retained activity for longer periods. A G $\alpha_{i1\text{-GDP}}$ aliquot was kept on ice and used within 30 min after thawing; longer storage on ice resulted in loss of activity (as assayed by the ability of 60 nM G $\alpha_{i1\text{-GDP}}$ to prevent activation of GIRK by 20 nM G $\beta\gamma$).

Biochemistry

The oocytes were homogenized on ice in homogenization buffer (20 mM Tris, pH 7.4, 5 mM EGTA, 5 mM EDTA, 100 mM NaCl) containing

the Roche Molecular Biochemicals protease inhibitor mixture. Debris was removed by centrifugation at $8000 \times g$ for 15 min at 4°C (Ivanina et al., 1994). For Western blots, protein samples were separated on 10% or 12% polyacrylamide-SDS gels. When necessary, total cellular membrane fraction from 5–17 oocytes was obtained by 1 hr centrifugation at $27,000 \times g$. Antibodies against $\text{G}\alpha_{13}$ (Calbiochem), $\text{G}\beta$ common (Santa Cruz), GIRK1, and GIRK2 (Alomone Labs., Jerusalem) were used. Visualization of protein bands was performed using ECL reagents obtained from Pierce Inc. Intensity of labeling was quantified using the TINA software (Raytest, Straubenhardt, Germany).

Immunoprecipitation of metabolically [^{35}S]-labeled GIRK channels was done as described (Ivanina et al., 1994). In brief, oocytes were incubated in NDE solution containing 0.5 mCi/ml [^{35}S]-methionine/cysteine (Amersham Pharmacia) for 3–4 days at 22°C . Plasma membranes were separated manually from the rest of the oocyte (designated as internal fraction). Five to ten membranes and three to five internal fractions, or five whole oocytes, were homogenized, proteins were solubilized, immunoprecipitated by the GIRK2 antibody, and electrophoresed on 10% polyacrylamide-SDS gel. The protein bands of the gel were imaged and quantitated using PhosphorImager (Molecular Dynamics) and the software ImageQuant.

The DNA sequence encoding the first 84 amino acids of GIRK1 was inserted between the EcoRI-NotI sites of the pGEX-4T-1 vector (Amersham Pharmacia Biotech), and the GST-fused protein, N_{1-84} , was synthesized according to manufacturer's instructions. $\text{G}\alpha_{13}$ and $\text{G}\beta\gamma$ were synthesized in reticulocyte lysate and labeled with [^{35}S]Met/Cys as described (Ivanina et al., 2000). Five microliters lysate was incubated for 30 min at 4°C in 95 μl of binding buffer (in mM: 50 Tris, 5 MgCl_2 , 1 EDTA, 0.05% Tween-20, pH 7.0, with 150 KCl) with 100 μM of either GDP or GTP- γS . Then 10 μg N_{1-84} was added, the total reaction volume brought to 300 μl , and the incubation continued in the presence of 100 μM GTP- γS or GDP for 1 to 2 hr at room temperature. Then glutathione Sepharose beads were added, incubated at 4°C for 30 min, and washed with the same buffer or with PBS but without the guanine nucleotides as described (Ivanina et al., 2000). The bound proteins were eluted with 15 mM glutathione and subjected to standard SDS-PAGE.

Confocal Imaging of Proteins in Large Plasma Membrane Patches

Devitalized oocytes were placed on coverslips, and after a few minutes, the outer side of the membrane adhered to the glass. The rest of the oocyte was then removed, leaving a large patch of plasma membrane on the coverslip with its inner surface exposed to the external solution (see Singer-Lahat et al., 2000 for details). The membranes were fixated, stained by specific antibodies, and visualized using a Cy3-conjugated rabbit IgG (Jackson Immunoresearch Laboratories) using the Zeiss LSM 410 confocal microscope. The total optical density (OD) of the image (which is proportional to the amount of the primary antibody and thus to the amount of the protein in the membrane) was measured using the TINA software.

Statistical Analysis

Data are presented as mean \pm SEM. Comparison between two groups of treatment was done using the two-tailed Student test. Comparison between several groups of data has been performed using one-way analysis of variance (ANOVA) followed by Student-Newman-Keuls or Dunnett's test. To enable averaging of the data across several oocyte batches, certain parameters were normalized as follows: one of the treatment groups was chosen as reference (e.g., 50 pg GIRK RNA). In each oocyte, the parameter under question was calculated as percent of the average parameter in the reference group, and then the data were averaged across all batches (Sharon et al., 1997).

Acknowledgments

We are grateful to the colleagues who kindly provided the original cDNA clones: E. Peralta (m2R), P. Kofuji and H. Lester (GIRK2), M. Simon (G protein subunits), E. Reuveny (c β ARK), E. Liman (pGEMHE), and L. Salkoff (pBS-MXT). We thank R. Barzilai for expert technical assistance, A. Mittelman and A. Barbul for help with confo-

cal microscopy, E. Reuveny for helpful suggestions, D. Singer-Lahat for advice in immunohistochemical and biochemical experiments, I. Lotan for the critical reading of the manuscript, and an anonymous reviewer for helpful and constructive critique. This work was supported by the NIH (GM 56260-01).

Received March 15, 2001; revised October 9, 2001.

References

- Bender, K., Wellner-Kienitz, M.C., Meyer, T., and Pott, L. (1998). Activation of muscarinic K^+ current by β -adrenergic receptors in cultured atrial myocytes transfected with $\beta 1$ subunit of heterotrimeric G proteins. *FEBS Lett.* 439, 115–120.
- Clapham, D.E., and Neer, E.J. (1997). G protein $\beta\gamma$ subunits. *Annu. Rev. Pharmacol. Toxicol.* 37, 167–203.
- Dascal, N. (1997). Signalling via the G protein-activated K^+ channels. *Cell.* 9, 551–573.
- Gilman, A.G. (1987). G proteins: transducers of receptor-generated signals. *Annu. Rev. Biochem.* 56, 615–649.
- He, C., Zhang, H., Mirshahi, T., and Logothetis, D.E. (1999). Identification of a potassium channel site that interacts with G protein $\beta\gamma$ subunits to mediate agonist-induced signaling. *J. Biol. Chem.* 274, 12517–12524.
- Hille, B. (1994). Modulation of ion-channel function by G-protein-coupled receptors. *Trends Neurosci.* 17, 531–536.
- Huang, C.L., Slesinger, P.A., Casey, P.J., Jan, Y.N., and Jan, L.Y. (1995). Evidence that direct binding of $\text{G}\beta\gamma$ to the GIRK1 G protein-gated inwardly rectifying K^+ channel is important for channel activation. *Neuron* 15, 1133–1143.
- Huang, C.L., Jan, Y.N., and Jan, L.Y. (1997). Binding of the G protein $\beta\gamma$ subunit to multiple regions of G protein-gated inward-rectifying K^+ channels. *FEBS Lett.* 405, 291–298.
- Ivanina, T., Perets, T., Thornhill, W.B., Levin, G., Dascal, N., and Lotan, I. (1994). Phosphorylation by protein kinase A of RCK1 K^+ channels expressed in *Xenopus* oocytes. *Biochemistry* 33, 8786–8792.
- Ivanina, T., Blumenstein, Y., Shistik, E., Barzilai, R., and Dascal, N. (2000). Modulation of L-type Ca^{2+} channels by $\text{G}\beta\gamma$ and calmodulin via interactions with N- and C-termini of α_{1C} . *J. Biol. Chem.* 275, 39846–39854.
- Ivanova-Nikolova, T.T., and Breitwieser, G.E. (1997). Effector contributions to $\text{G}\beta\gamma$ -mediated signaling as revealed by muscarinic potassium channel gating. *J. Gen. Physiol.* 109, 245–253.
- Jelacic, T.M., Sims, S.M., and Clapham, D.E. (1999). Functional expression and characterization of G-protein-gated inwardly rectifying K^+ channels containing GIRK3. *J. Membr. Biol.* 169, 123–129.
- Kim, D., Watson, M., and Indyk, V. (1997). ATP-dependent regulation of a G protein-coupled K^+ channel (GIRK1/GIRK4) expressed in oocytes. *Am. J. Physiol.* 272, H195–H206.
- Kozasa, T., Kaziro, Y., Ohtsuka, T., Grigg, J.J., Nakajima, S., and Nakajima, Y. (1996). G protein specificity of the muscarine-induced increase in an inward rectifier potassium current in AtT-20 cells. *Neurosci. Res.* 26, 289–297.
- Krapivinsky, G., Gordon, E.A., Wickman, K., Velimirovic, B., Krapivinsky, L., and Clapham, D.E. (1995). The G-protein-gated atrial K^+ channel I_{KACH} is a heteromultimer of two inwardly rectifying K^+ -channel proteins. *Nature* 374, 135–141.
- Krapivinsky, G., Kennedy, M.E., Nemecek, J., Medina, I., Krapivinsky, L., and Clapham, D.E. (1998). $\text{G}\beta$ binding to GIRK4 subunit is critical for G protein-gated K^+ channel activation. *J. Biol. Chem.* 273, 16946–16952.
- Leaney, J.L., and Tinker, A. (2000). The role of members of the pertussis toxin-sensitive family of G proteins in coupling receptors to the activation of the G protein-gated inwardly rectifying potassium channel. *Proc. Natl. Acad. Sci. USA* 97, 5651–5656.
- Leaney, J.L., Milligan, G., and Tinker, A. (2000). The G protein α subunit has a key role in determining the specificity of coupling to,

- but not the activation of, G protein-gated inwardly rectifying K⁺ channels. *J. Biol. Chem.* 275, 921–929.
- Lei, Q., Jones, M.B., Talley, E.M., Schrier, A.D., McIntire, W.E., Garrison, J.C., and Bayliss, D.A. (2000). Activation and inhibition of G protein-coupled inwardly rectifying potassium (Kir3) channels by G protein $\beta\gamma$ subunits. *Proc. Natl. Acad. Sci. USA* 97, 9771–9776.
- Lesage, F., Guillemare, E., Fink, M., Duprat, F., Heurteaux, C., Fosset, M., Romey, G., Barhanin, J., and Lazdunski, M. (1995). Molecular properties of neuronal G-protein-activated inwardly rectifying K⁺ channels. *J. Biol. Chem.* 270, 28660–28667.
- Lim, N.F., Dascal, N., Labarca, C., Davidson, N., and Lester, H.A. (1995). A G protein-gated K channel is activated via β_2 -adrenergic receptors and G $\beta\gamma$ subunits in *Xenopus* oocytes. *J. Gen. Physiol.* 105, 421–439.
- Logothetis, D.E., and Zhang, H. (1999). Gating of G protein-sensitive inwardly rectifying K⁺ channels through phosphatidylinositol 4,5-bisphosphate. *J. Physiol. (Lond.)* 520, 630.
- Lutz, L.B., Kim, B.E., Jahani, D., and Hammes, S.R. (2000). G protein $\beta\gamma$ subunits inhibit nongenomic progesterone-induced signaling and maturation in *Xenopus* oocytes: evidence for a release of inhibition mechanism for cell cycle progression. *J. Biol. Chem.* 275, 41512–41520.
- Nemec, J., Wickman, K., and Clapham, D.E. (1999). G $\beta\gamma$ binding increases the open time of I_{KACH}: kinetic evidence for multiple G $\beta\gamma$ binding sites. *Biophys. J.* 76, 246–252.
- Petit-Jacques, J., Sui, J.L., and Logothetis, D.E. (1999). Synergistic activation of G protein-gated inwardly rectifying potassium channels by the $\beta\gamma$ subunits of G proteins and Na⁺ and Mg²⁺ ions. *J. Gen. Physiol.* 114, 673–684.
- Reuveny, E., Slesinger, P.A., Inglese, J., Morales, J.M., Iniguez-Lluhi, J.A., Lefkowitz, R.J., Bourne, H.R., Jan, Y.N., and Jan, L.Y. (1994). Activation of the cloned muscarinic potassium channel by G protein $\beta\gamma$ subunits. *Nature* 370, 143–146.
- Ross, E.M. (1995). G protein GTPase-activating proteins: regulation of speed, amplitude, and signaling selectivity. *Recent Prog. Horm. Res.* 50, 207–221.
- Sadja, R., Smadja, K., Alagem, N., and Reuveny, E. (2001). Coupling G $\beta\gamma$ -dependent activation to channel opening via pore elements in inwardly rectifying potassium channels. *Neuron* 29, 669–680.
- Sakmann, B., Noma, A., and Trautwein, W. (1983). Acetylcholine activation of single muscarinic K⁺ channels in isolated pacemaker cells of the mammalian heart. *Nature* 303, 250–253.
- Sarvazyan, N.A., Remmers, A.E., and Neubig, R.R. (1998). Determinants of G β_1 and $\beta\gamma$ binding. Measuring high affinity interactions in a lipid environment using flow cytometry. *J. Biol. Chem.* 273, 7934–7940.
- Schreibmayer, W., Dessauer, C.W., Vorobiov, D., Gilman, A.G., Lester, H.A., Davidson, N., and Dascal, N. (1996). Inhibition of an inwardly rectifying K⁺ channel by G-protein α subunits. *Nature* 380, 624–627.
- Sharon, D., Vorobiov, D., and Dascal, N. (1997). Positive and negative coupling of the metabotropic glutamate receptors to a G protein-activated K⁺ channel, GIRK, in *Xenopus* oocytes. *J. Gen. Physiol.* 109, 477–490.
- Singer-Lahat, D., Dascal, N., Mittelman, L., Peleg, S., and Lotan, I. (2000). Imaging plasma membrane proteins in large membrane patches of *Xenopus* oocytes. *Pflugers Arch.* 440, 627–633.
- Sorota, S., Rybina, I., Yamamoto, A., and Du, X.Y. (1999). Isoprenaline can activate the acetylcholine-induced K⁺ current in canine atrial myocytes via Gs-derived $\beta\gamma$ subunits. *J. Physiol. (Lond.)* 514, 413–423.
- Sowell, M.O., Ye, C., Ricupero, D.A., Hansen, S., Quinn, S.J., Vassilev, P.M., and Mortensen, R.M. (1997). Targeted inactivation of α_{12} or α_{13} disrupts activation of the cardiac muscarinic K⁺ channel, I_{KACH}, in intact cells. *Proc. Natl. Acad. Sci. USA* 94, 7921–7926.
- Sui, J.L., Petit-Jacques, J., and Logothetis, D.E. (1998). Activation of the atrial KACH channel by the $\beta\gamma$ subunits of G proteins or intracellular Na⁺ ions depends on the presence of phosphatidylinositol phosphates. *Proc. Natl. Acad. Sci. USA* 95, 1307–1312.
- Sunahara, R.K., Dessauer, C.W., and Gilman, A.G. (1996). Complexity and diversity of mammalian adenylyl cyclases. *Annu. Rev. Pharmacol. Toxicol.* 36, 461–480.
- Vorobiov, D., Bera, A.K., Keren-Raifman, T., Barzilai, R., and Dascal, N. (2000). Coupling of the muscarinic m2 receptor to G protein-activated K⁺ channels via G α_z and a receptor-G α_z fusion protein. Fusion between the receptor and G α_z eliminates catalytic (collision) coupling. *J. Biol. Chem.* 275, 4166–4170.
- Wickman, K., and Clapham, D.E. (1995). Ion channel regulation by G proteins. *Physiol. Rev.* 75, 865–885.
- Wickman, K.D., Iniguez-Lluhi, J.A., Davenport, P.A., Taussig, R., Kravinsky, G.B., Linder, M.E., Gilman, A.G., and Clapham, D.E. (1994). Recombinant G-protein $\beta\gamma$ -subunits activate the muscarinic-gated atrial potassium channel. *Nature* 368, 255–257.
- Yakubovich, D., Pastushenko, V., Bitler, A., Dessauer, C.W., and Dascal, N. (2000). Slow modal gating of single G protein-activated K⁺ channels expressed in *Xenopus* oocytes. *J. Physiol. (Lond.)* 524, 737–755.
- Yamada, M., Inanobe, A., and Kurachi, Y. (1998). G protein regulation of potassium ion channels. *Pharmacol. Rev.* 50, 723–757.
- Yi, B.A., Lin, Y., Jan, Y.N., and Jan, L.Y. (2001). Yeast screen for constitutively active mutant G protein-activated potassium channels. *Neuron* 29, 657–667.